SCIENCE CHINA
Earth Sciences

• RESEARCH PAPER •

November 2014 Vol.57 No.11: 2628–2636
doi: 10.1007/s11430-014-4949-6

Relationship between zonal position of the North Atlantic Oscillation and Euro-Atlantic blocking events and its possible effect on the weather over Europe

YAO Yao[1,2] & LUO DeHai[2*]

[1] *Physical Oceanography Laboratory, College of Physical and Environmental Oceanography, Ocean University of China, Qingdao 266100, China;*
[2] *RCE-TEA, Institute of Atmospheric Physics, Chinese Academy of Sciences, Beijing 100029, China*

Received July 1, 2013; accepted November 27, 2013; published online September 12, 2014

The North Atlantic Oscillation (NAO) exhibited a marked eastward shift in the mid-1970s. Observations show that the extreme weather events in Europe have emerged frequently in the past decades. In this paper, based upon the daily NAO index, we have calculated the frequency of *in-situ* NAO events in winter during 1950−2011 by defining the Eastern-type NAO (ENAO) and Western-type NAO (WNAO) events according to its position at the east (west) of 10°W. Then, the composites of the blocking frequency, temperature and precipitation anomalies for different types of NAO events are performed. Results show that the frequency of Euro-Atlantic blocking events is distributed along the northwest-southeast (southwest-northeast) direction for the negative (positive) phase. Two blocking action centers in Greenland and European continent are observed during the negative phase while one blocking action center over south Europe is seen for the positive phase. The action center of blocking events tends to shift eastward as the NAO is shifted toward the European continent. Moreover, the eastern-type negative phase ($ENAO^-$) events are followed by a sharp decline of surface air temperature over Europe (especially in central, east, and south Europe), which have a wider and stronger impact on the weather over European continent than the western-type negative phase ($WNAO^-$) events do. A double- branched structure of positive precipitation anomalies is seen for the negative phase event, besides strong positive precipitation anomalies over south Europe for $ENAO^-$ event. The eastern-type and western-type positive phase ($ENAO^+$ and $WNAO^+$) can lead to warming over Europe. A single-branched positive precipitation anomaly dominant in central and north Europe is seen for positive phase events.

North Atlantic Oscillation, atmospheric blocking, temperature, precipitation

Citation: Yao Y, Luo D H. 2014. Relationship between zonal position of the North Atlantic Oscillation and Euro-Atlantic blocking events and its possible effect on the weather over Europe. Science China: Earth Sciences, 57: 2628−2636, doi: 10.1007/s11430-014-4949-6

The North Atlantic Oscillation (NAO), one of the most prominent low-frequency variability in the Northern Hemisphere, has become an interesting research topic because of its important impact on the decadal variability and global warming in recent several decades. Walker first proposed the definition of NAO at the beginning of the twentieth century (Walker, 1924; Walker and Bliss, 1932). The temporal and spatial variations of NAO can modulate weather and climate not only in Euro-Atlantic but also in its adjacent regions and even over the whole Northern Hemisphere (Hurrell, 1995). It has been revealed that cooling over Europe is observed for the negative phase of NAO (NAO^-), but warming for the positive phase of NAO (NAO^+) cycle (Hurrell, 1996).

*Corresponding author (email: ldh@mail.iap.ac.cn)

Many investigations indicate that the abnormal circulation of NAO may motivate extreme weather in Europe and surrounding areas. The NAO^- is usually associated with extreme cold and blizzard events in Europe. Sillmann and Croci-Maspoli (2009) found that the cold events in Europe are associated with not only the phases of NAO but also the Europe blocking activity. Wang et al. (2010) indicated that the extreme cold winter in 2009/2010 was related to the extreme abnormal NAO circulation, which transported the cold air from Arctic to southern area. Li et al. (2011) examined the extreme weather in the Northern Hemisphere in 2009/2010 winter and suggested that the abnormal temperature and precipitation were closely related to the notable negative Arctic Oscillation (AO) phase.

Many studies suggested that the global drought and flood in China are associated with not only NAO, AO, North Pacific Oscillation (NPO), and blocking but also Antarctic Oscillation (AAO), Southern Hemisphere Annular Mode (SAM), and Atlantic Multidecadal Oscillation (AMO) (Li and Li, 1999; Fan and Wang, 2006; Ma and Fu, 2007; Wang et al., 2007; Li and Bates, 2007; Sun et al., 2008; Zhou et al., 2008, 2013; Li et al., 2009; Wei and Zhang, 2009; Wu et al., 2009; Xu et al., 2012; He et al, 2013). Fu and Zeng (2005) showed that the NAO index of the past 530 years has a good delay correlation with several drought indices in Eastern China. Wu et al. (1999, 2005) noted that the NAO and AO may adjust the weather in China during winter time by affecting the Arctic Sea ice and winter monsoon. Recently, it was noted that the extreme cold event in China was closely related to the synoptic transient eddy activity in the Ural Mountain, which can be influenced by NAO, blocking, and mid-high latitude jet (Chen et al., 2012).

Many studies indicated that the Euro-Atlantic blocking can be influenced by the phases of NAO (Shabbar et al., 2001; Scherrer et al., 2006; Croci-Maspoli and Schwierz, 2007). Using a weakly non-linear theoretical model, Luo et al. (2007c) found that the enhanced zonal wind in the Atlantic will excite a strong downstream dispersion of the Rossby wave during the life cycle of NAO, which resulted in the enhanced occurrence frequency of Europe blocking. Furthermore, a marked eastward shift of the NAO since the 1970s is observed by observational and numerical study (Hilmer and Jung, 2000; Jung et al., 2003; Luo and Gong, 2006; Dong et al., 2010; Zhang et al., 2011). However, it is still unclear whether the frequent occurrence of the extreme weather in Europe is related to the eastward shift of NAO and Europe blocking. The purpose of this paper is to reveal the differences between the Eastern-type NAO (ENAO) and Western-type NAO (WNAO) events, including associated blocking, temperature and precipitation. The investigation of this topic will help us to understand the role of the NAO variability in the occurrence of extreme weather in Europe.

1 Data and methods

1.1 Data

The data set we use is the multi-level daily reanalysis data on a 2.5°×2.5° horizontal resolution from NCEP/NCAR during the period from November 1950 to March 2012. The European daily surface temperature and precipitation gridded dataset is obtained from the European Climate Center (ECAD) (http://eca.knmi.nl/), with a 0.5°×0.5° horizontal resolution from November 1950 to March 2012. The daily NAO index used for identifying NAO events is constructed by projecting the daily 500 hPa height anomalies over the Northern Hemisphere onto the loading pattern of the NAO, which can be available from the Climate Prediction Center (CPC) of NOAA (http://www.cpc.noaa.gov) and referred to as the CPC NAO index hereafter. In this study, the winter period is defined as a time interval from November to March (NDJFM). The intraseasonal cycle has been removed during the calculating of the anomaly data.

1.2 Methods

According to Luo et al. (2012a, 2012b, 2012c), the NAO events are divided into *in-situ* NAO and transition NAO events. Specifically, an NAO^+ (NAO^-) event is identified if the normalized daily NAO index is larger (less) than +1.0 (−1.0) standard deviation for at least 3 continuous days. The life cycle of an NAO^+ (NAO^-) event is defined to be between the starting with an increase (a decrease) in the NAO index and ending with a decrease (an increase) in the NAO index. The time of the strongest NAO amplitude is defined as the lag 0 day. The definition of the *in-situ* NAO event is that one NAO event is not followed by an opposite NAO phase event within 5 days and its total life cycle does not exceed 30 days. A transition event is defined to include two opposite NAO events and its total days do not exceed 45 days (Luo et al., 2012a, 2012b). The time interval between the peaks of the two opposite events does not exceed 30 days. Only the impact of *in-situ* NAO event is dealt with here owing to the limitation of space.

To identify blocking activity in Euro-Atlantic area, a two-dimensional blocking index (Davini et al., 2012a, 2012b) is used here based upon the one-dimensional blocking index (Tibaldi and Molteni, 1990). The two-dimensional blocking index identifies the blocking events by examining the meridional gradient reversal of the 500 hPa geopotential height. The steps are as follows:

$$\mathrm{GHGS}\ (\lambda_0,\phi_0)=\frac{Z(\lambda_0,\phi_0)-Z(\lambda_0,\phi_S)}{\phi_0-\phi_S}, \tag{1a}$$

$$\mathrm{GHGN}\ (\lambda_0,\phi_0)=\frac{Z(\lambda_0,\phi_N)-Z(\lambda_0,\phi_0)}{\phi_N-\phi_0}, \tag{1b}$$

where Z (λ_0, ϕ_0) is the 500 hPa geopotential height at grid

point (λ_0, ϕ_0), λ_0 (ϕ_0) represents the position of longitude (latitude) and ranges from 0° to 360° (30° to 70°N); $\phi_N=\phi_0+15°$, $\phi_s=\phi_0-15°$

$$\text{GHGS}\ (\lambda_0,\phi_0)>0, \quad \text{GHGN}\ (\lambda_0,\phi_0)<-10\ \text{m/°lat}. \quad (2)$$

For the grid point $Z(\lambda_0, \phi_0)$, an instantaneous blocking (IB) event is considered to have taken place if the constraint condition (2) is satisfied.

2 The zonal position of NAO and its impact on Euro-Atlantic blocking

2.1 Eastern and western types of NAO events

There are two phases of NAO events: *in-situ* NAO^+ and *in-situ* NAO^- events (NAO^+ and NAO^- hereafter). The NAO events including NAO^+ and NAO^- during the period from 1950/1951 to 2011/2012 winter time are identified based upon the daily CPC NAO index. Usually, the southern center of the NAO dipole mode has a larger longitude range and multiple-value centers while its northern anomaly has a single- value center in high latitude. It is reasonable to divide NAO events into eastern- and western-type events according to the zonal position of northern center of the NAO dipole mode. The NAO events whose north centers (at the day lag 0) are located in the east (west) of 10°W are defined as eastern- (western-) type NAO events (ENAO and WNAO events, hereafter). As listed in Table 1, and the number of ENAO events is about one quarter of the number of WNAO events. The numbers of $ENAO^+$ ($ENAO^-$) events account for 21.6% (18.2%) of NAO^+ (NAO^-) events.

Table 1 Number of ENAO and WNAO events in winter during the period from 1950 to 2012

Phases\Number	1950–2011 winter time		
	NAO	ENAO	WNAO
NAO^+	97	21	76
NAO^-	99	18	81

The time series of the NAO event and day numbers in winter time are shown in Figure 1(a), (b). Results show that the time series of the NAO event and day numbers exhibit the same variability with the NAO index during the period from 1950 to 2012. Furthermore, it is suggested that there are no significant differences (below the 95% confidence level for a Monte-Carlo test) between composites of the ENAO and WNAO events index. Therefore, the zonal locations of the ENAO and WNAO events cannot be reflected by the NAO index because it mainly reflects the latitudinal variation of dipole modes. However, the significant impact on Europe weather due to the zonal shift of the NAO pattern needs to be further examined.

2.2 Blocking and circulation associated with the ENAO and WNAO events

To understand the variability of blocking activity during the ENAO and WNAO life cycle, the blocking distribution is calculated based upon the two-dimension index (Davini et al., 2012a, 2012b). Figure 2 shows the occurrence frequency

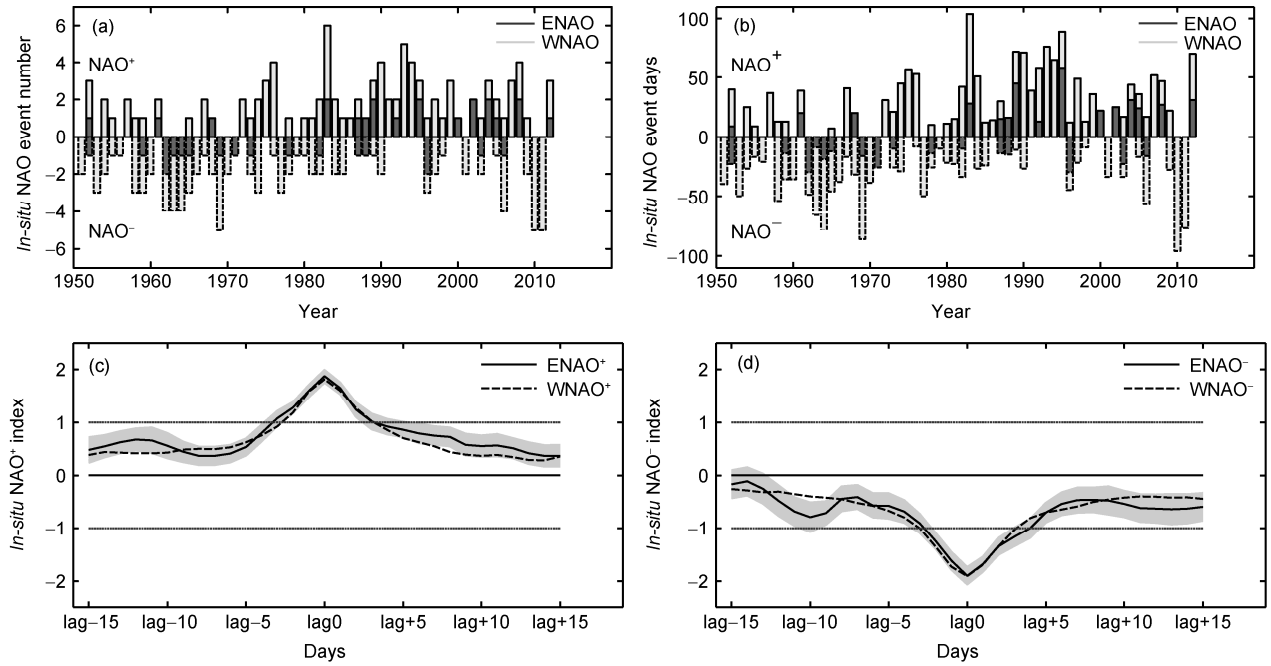

Figure 1 Time series of the number (a) and days (b) of the NAO events during winter time from 1950 to 2011 in which the dark (light) bar represents the ENAO (WNAO) events. Composites of the NAO indices for NAO^+ and NAO^- events are shown in (c) and (d). The solid (dotted) line represents the ENAO (WNAO) events. The gray shaded indicates the region below the 95% confidence level for a Monte-Carlo test.

of blocking days in the Euro-Atlantic area. The blocking frequency distribution of NAO^+ events is from the eastern Atlantic to northern Europe with a center in southwest Europe. This structure can be called a southwest-northeast (WS-NE) structure (Figure 2(a)). For NAO^- events, the blocking frequency presents a northwest-southeast (WN-SE) structure, which has two centers located near Greenland and southwest Europe, respectively (Figure 2(b)). The blocking frequency distributions of ENAO and WNAO events are shown in Figure 3. The blocking action center of the $ENAO^+$ (Figure 3(b)) is located closer to European continent (especially over south Europe) than that of $ENAO^-$ (Figure 3(a)). The blocking activity of $ENAO^-$ events (Figure 3(d)) covers much of European continent and Greenland. The blocking activity of $WNAO^-$ events is located more westward than $ENAO^-$ events (Figure 3(c)). It is found that the blocking events are more frequent in European continent (Atlantic) during the NAO^+ (NAO^-) life cycle, which is consistent with previous studies (Shabbar et al., 2001; Luo et al., 2007a, 2007b, 2007c; Woollings et al., 2008).

To further understand the difference of blocking between ENAO and WNAO events, the composites of 500 hPa geopotential height anomalies averaged from lag–5 to lag+5 of an NAO life cycle are presented in Figure 4. It is shown that the negative anomaly center of the NAO^+ dipole modes is located within the domain from 60° to 30°W. The positive anomaly center of the NAO^- dipole modes is located from 60° W to 0° (Figure 4(a)). For NAO^- events, the positive anomaly center is located from 60° to 40°W and negative anomaly center is located from 60°W to 0° (Figure 4(b)). Moreover, the dipole modes of the ENAO events are located more eastward than WNAO events (Figure 5). Figure 5(b) shows that the negative anomaly center of $ENAO^+$ has a marked eastward shift and extends to the east of 0°. For $ENAO^-$ events (Figure 5(d)), and the positive anomaly center is located in east of the North Atlantic and covers much

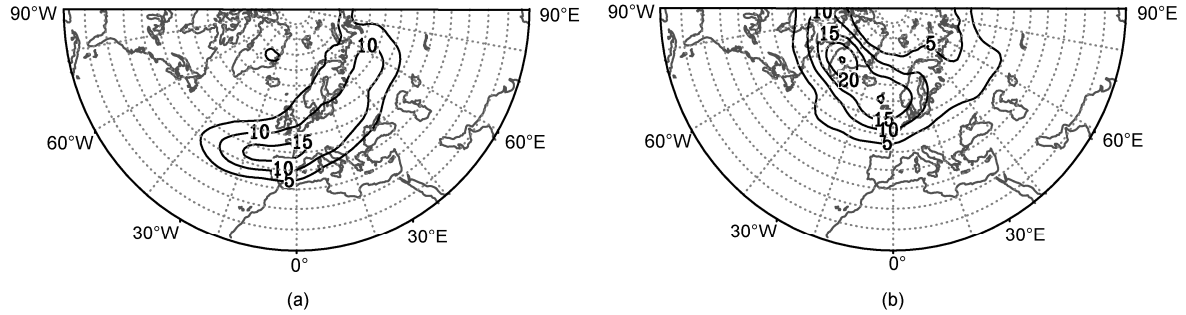

Figure 2 Composites of the instantaneous blocking frequencies for NAO^+ (a) and NAO^- (b) events averaged from lag-5 to lag+5 during the NAO life cycle. The units are % and the contours are drawn from 5 to 25 with 5 intervals. The latitude lines are at 5° intervals starting with 20°N at the edges.

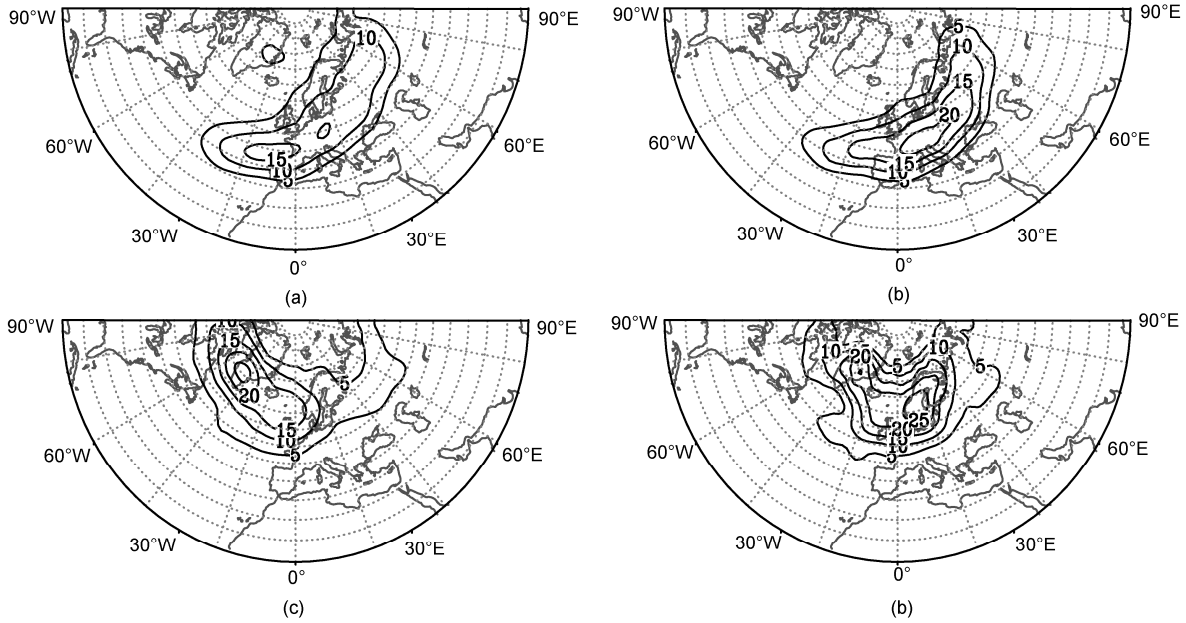

Figure 3 Composites of the instantaneous blocking frequencies for $WNAO^+$ (a), $ENAO^-$ (b), $WNAO^-$ (c), and $ENAO^-$ (d) events averaged from lag-5 to lag+5 during the NAO life cycle. The units are % and the contours are drawn from 5 to 25 with 5 intervals. The latitude lines are at 5° intervals starting with 20°N at the edges.

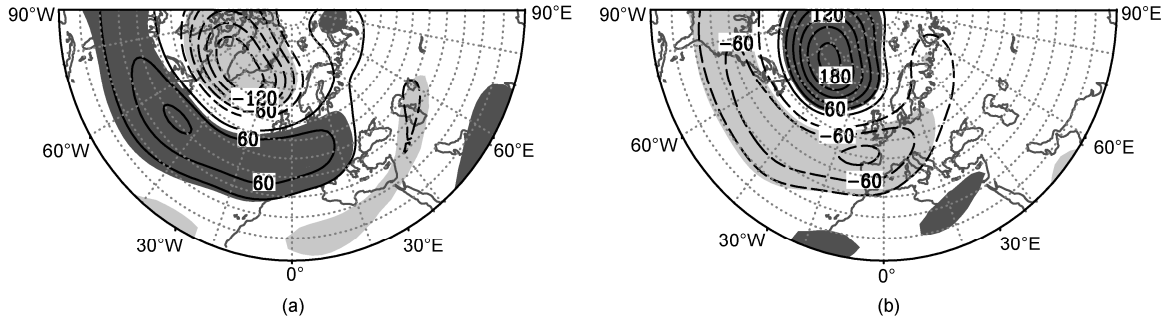

Figure 4 Composites of the 500 hPa geopotential height anomalies for NAO^+ (a) and NAO^- (b) events averaged during the lag−5 to lag+5 of NAO life cycle. The units are gpm and the contours are drawn from 30 to 180 with 30 intervals. The latitude lines are at 5° intervals starting with 20°N at the edges. Dark (light) shading indicates the contours of positive (negative) anomalies exceed the 95% confidence level for a two-sided Student *t*-test.

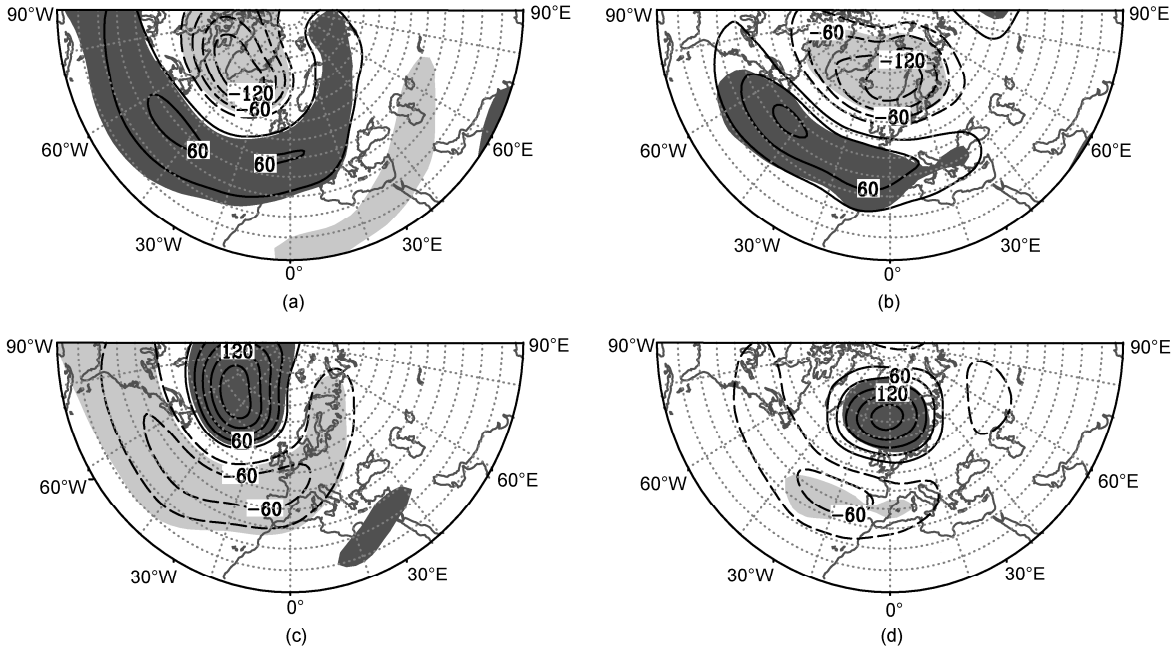

Figure 5 Composites of the 500 hPa geopotential height anomalies for $WNAO^+$ (a), $ENAO^-$ (b), $WNAO^-$ (c), and $ENAO^-$ (d) events averaged from lag−5 to lag+5 during the NAO life cycle. The units are gpm and the contours are drawn from 30 to 180 with 30 intervals. The latitude lines are plotted with 5° intervals starting with 20°N at the edges. Dark (light) shading indicates the contours of positive (negative) anomalies exceed the 95% confidence level for a two-sided Student *t*-test.

of the northwest European continent. It suggests that the blocking activity in Euro-Atlantic area can reflect the zonal position of NAO events.

2.3 Temperature and precipitation associated with the ENAO and WNAO events

Figure 6 shows the distribution of surface temperature anomaly during the NAO life cycle in European continent. A marked positive (negative) temperature anomaly can be observed during the NAO^+ (NAO^-) life cycle in European continent (Figure 6). It is found that the positive temperature anomaly presents a southwest-northeast structure (see significant lines above the 95% confidence level for a two-sided Student's *t*-test in Figure 6(a) and (b) during the NAO^+ life cycle. And a notable positive temperature anomaly can be observed in central and eastern European continent during $ENAO^+$ life cycle (Figure 6(b)). To the contrary, a negative temperature anomaly is found over Europe during the life cycle of NAO^- events. Moreover, a marked negative temperature anomaly is observed in southeast Europe during $ENAO^-$ events (Figure 6(d)). It suggests that the eastward shift of the NAO events has a greater influence on the European temperature. It means that marked and widespread decline (rise) of temperature can be seen over Europe if NAO^- (NAO^+) dipole mode is located closer to European continent. It is worth noting that although the temperature anomalies are different between $WNAO^+$ and $EANO^+$ events, the same SW-NE structure can be observed. Moreover, the positive temperature anomaly center in $ENAO^+$ events is located more southward and is more widespread than $WNAO^+$ events (Figure 7(a), (b)). The

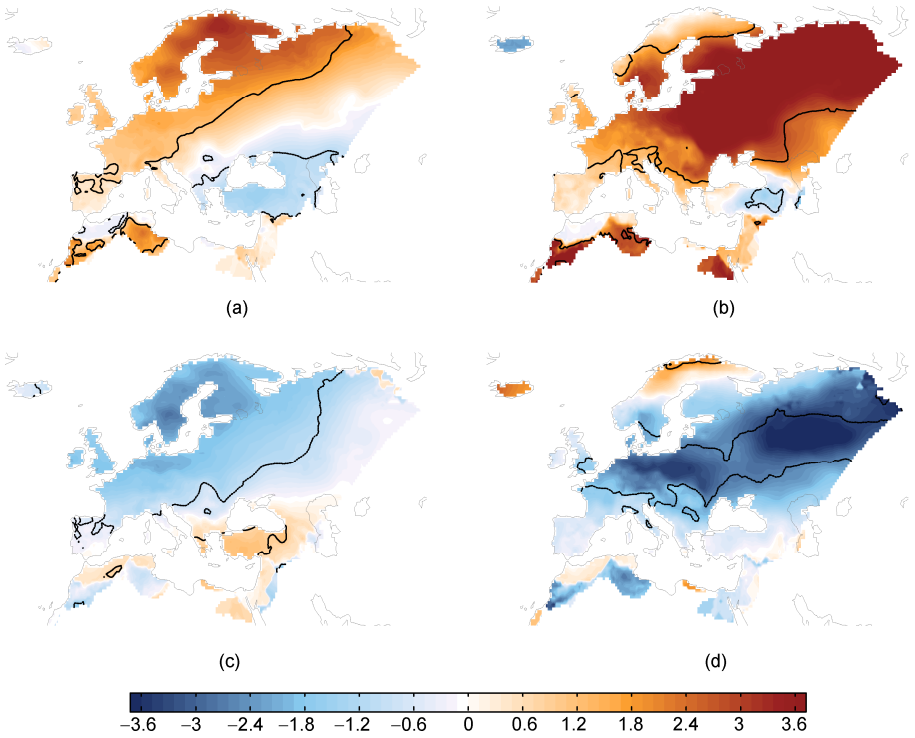

Figure 6 Composites of the surface temperature anomaly for $WNAO^{+}$ (a), $ENAO^{-}$ (b), $WNAO^{-}$ (c), and $ENAO^{-}$ (d) events averaged from lag−5 to lag+5 during the NAO life cycle. The units are °C. Solid (dotted) line indicates the shading of positive (negative) anomalies exceed the 95% confidence level for a two-sided Student *t*-test.

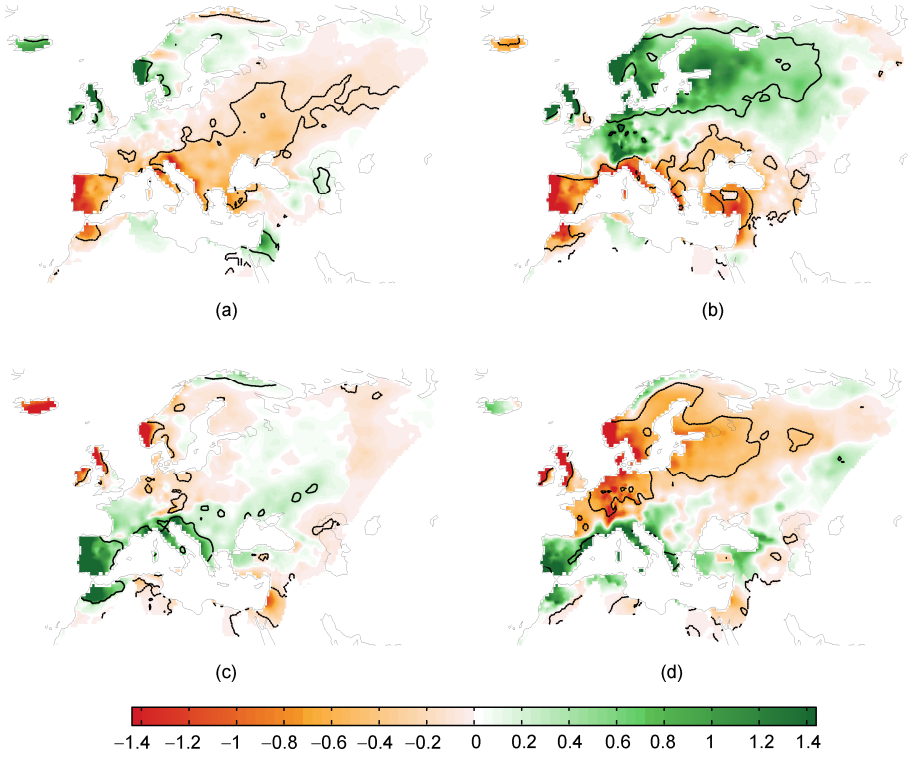

Figure 7 Composites of the surface precipitation anomaly for $WNAO^{+}$ (a), $ENAO^{-}$ (b), $WNAO^{-}$ (c), and $ENAO^{-}$ (d) events averaged from lag−5 to lag+5 during the NAO life cycle. The units are mm. Solid (dotted) line indicates the shading of positive (negative) anomalies exceed the 95% confidence level for a two-sided Student *t*-test.

same SW-NE structure is also seen in ENAO$^-$ and WNAO$^-$ (Figure 7(c), (d)). The most prominent negative temperature region during the ENAO$^-$ events is located in southeast Europe and even in the Mediterranean Sea (Figure 7(d)). It means that extreme cold events take place easily in Europe especially in southeast Europe during the life cycle of ENAO$^-$ events.

3 The possible mechanism of the ENAO events and its impact on Europe weather

3.1 The possible mechanism of the ENAO events

To further examine the mechanism of the occurrence of ENAO and WNAO events and their impact on Euro-Atlantic blocking. The latitudinal distribution of the time-mean zonal wind during the ENAO and WNAO events is presented in Figure 8. The time-mean is calculated for the period from lag−15 to lag−5 of the NAO life cycle. This period represents the early stage before the beginning of NAO events and a zonal average is made in the Atlantic area (60°W–0°).

As shown in Figure 8(a), (b), the zonal wind in the Atlantic area for ENAO events is stronger in mid-high latitude (40°–70°N) than WNAO events. Moreover, the results for the zonal wind averaged during the period from lag−5 to lag+5 are basically in agreement with those in Figure 8 (not shown). This suggests that the action center of NAO events may shift more eastward if the zonal wind in mid-high latitude is stronger (Luo et al., 2006). It indicates that the zonal positions of ENAO and WNAO events are influenced by the strength of the zonal wind. It means that the mean position of NAO dipole mode may undergo a westward migration if the zonal wind is weak. On the contrary, the westward migration is suppressed and even the eastward migration can be observed if the zonal wind is strong enough.

3.2 The storm track associated with the NAO events

According to the theoretical result by Luo et al. (2007a, 2007b, 2007c), a sketch map is presented to explain the relationship between the phases of NAO and storm track (Figure 9). It suggests that the NAO$^-$ is actually a blocking (meridional) circulation in the Atlantic area. The zonal wind and storm track are split into two (northern and southern) branches due to the feedback of the blocking (Figure 9(a)). And the precipitation, which is associated with the splitting of storm track, also exhibits a double-branched structure in Europe (Figure 7(c), (d)). For the ENAO$^-$ events, the bifurcation point of zonal wind and storm track is closer to the European continent and tends to have greater impacts on Europe weather. On the contrary, for the WNAO$^-$ events, their impacts on European weather are weak as a result of the upstream splitting of the zonal wind and storm track. The NAO$^-$ dipole mode is a high-over-low meridional structure in mid-high latitudes, which brings dry (moist) and

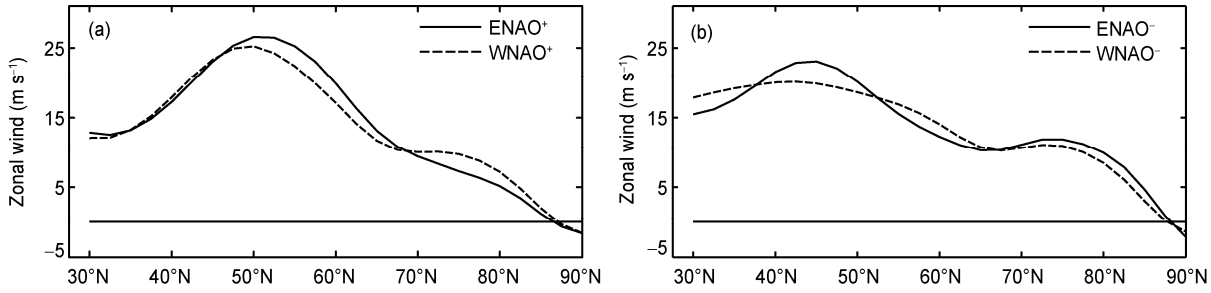

Figure 8 Meridional distribution of time-mean zonal wind from lag−15 to lag−5 at 300 hPa averaged over Atlantic region (60°W−0°) for NAO+ (a) and NAO$^-$ (b) events. The units are m s^{-1}.

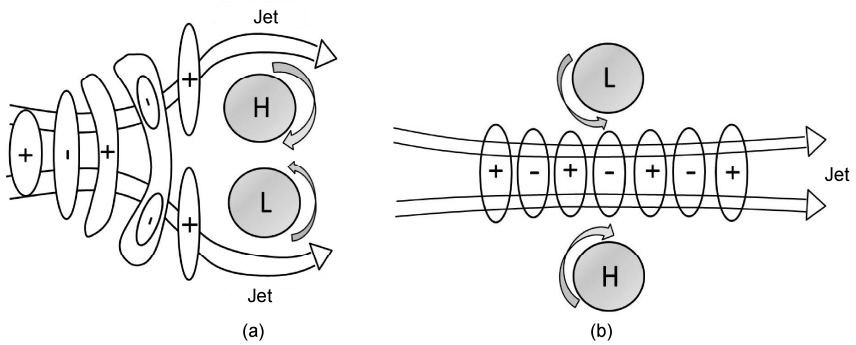

Figure 9 Schematics of the NAO circulation and associated storm track for NAO$^-$ (a) and NAO$^+$ (b) events.

cold (warm) air from Arctic (Atlantic) to mid-low (mid-high) latitude area. The impact of $ENAO^-$ events on temperature decline of European continent is prominent, especially in southeast Europe. For the NAO^+ events, the zonal wind, storm track and precipitation anomaly are a single-branched structure in central Europe (Figure 7(a), (b)).

4 Discussions and conclusion

In this paper, based upon the daily NAO index and definition of NAO events, all the *in-situ* NAO^+ and NAO^- events are identified during the period from 1950/1951 to 2011/2012 winter (NDJFM). In addition, the eastern-type (ENAO) and western-type NAO (WNAO) events are defined based upon the zonal position of the north center of NAO dipole mode. The distributions of blocking frequency, geopotential height anomalies, temperature, and precipitation anomalies during the ENAO and WNAO life cycle are further examined.

Results show that in the maturity stage of NAO life cycle, the mean amplitude of $ENAO^+$ events is stronger than that of $WNAO^+$ events. There is no evident difference of the composite geopotential height anomaly between $ENAO^-$ and $WNAO^-$ events. Moreover, the blocking activity of ENAO ($ENAO^+$ and $WNAO^-$) events is located more eastward than WNAO events ($WNAO^+$ and $WNAO^-$). For the NAO^+ (NAO^-) events, the distribution of the blocking activity is referred to as a WS-NE (WN-SE) structure.

It is found that the positive (negative) temperature anomaly in Europe during $ENAO^+$ ($ENAO^-$) events is larger and wider than $WNAO^+$ ($WNAO^-$) events. It is worth noting that the positive temperature anomaly can extend to the Mediterranean Sea and western Russia during the $ENAO^-$ life cycle. The positive precipitation anomaly presents a single-branched structure in central Europe during the NAO^+ events. For the NAO^- events, the positive precipitation anomaly presents a double-branched structure with a north branch along northern Europe and a south branch along southern Europe. The positive precipitation anomaly for $ENAO^+$ events is stronger and more widespread in central and north Europe than that for $WNAO^+$ events. Almost the same positive precipitation anomaly structure (double-branched) can be observed for $ENAO^-$ and $WNAO^-$ events. The marked persistent decline of temperature in southern Europe especially in the north shore of the Mediterranean Sea may cause extreme snowfall events in this area.

In addition, it is found that the zonal position of NAO dipole modes may be associated with the strength of the zonal wind. The double-branched structure of the positive precipitation anomaly for NAO^- events is likely to be controlled by the double-branched storm tracks. The southward transport of cold airs during the $ENAO^-$ life cycle may create a suitable condition for the cold weather occurrence in Europe.

In this study, we have examined the difference between ENAO and WNAO events and their impact on Europe weather. In order to reduce the subjectivity in the classification of ENAO and WNAO events, we have looked at the results for two criterions based on the NAO patterns centered at 10° and 20°W in our analysis. Moreover, the positive anomaly center of the dipole modes is also used to classify the NAO types. The results are qualitatively consistent (not shown).

Although the possible impacts of the ENAO and WNAO events are considered here, and the dynamical process of the NAO is still a front edge in Atmospheric research. It is possible to predict the occurrence of extreme weather if the NAO life cycle can be predicted. Recently, Jiang et al. (2013) applied the conditional non-linear optimal perturbations (CNOP) proposed by Mu et al. (Mu and Zhang, 2006; Mu and Jiang, 2007; Jiang et al., 2008) on the study of NAO dynamical process. This provided an important approach for the prediction of strong nonlinear system like NAO. This latter point will be an important work to be launched in the near future.

This work was supported by the National Natural Science Foundation of China (Grant No. 41375067) and we thank the anonymous reviewers for their comments which have improved the paper.

Chen H S, Liu L, Zhu Y J. 2012. Possible linkage between winter extreme low temperature events over China and synoptic-scale transient wave activity. Sci China Earth Sci, 56: 1266–1280

Fan K, W H J. 2006. Interannual variability of Antarctic Oscillation and its influence on East Asian climate during boreal winter and spring. Sci China Ser D-Earth Sci, 49: 554–560

Fu C B, Zeng Z M. 2005. The relationship between winter North Atlantic Oscillation index and summer eastern China dryness/wetness index in recent 530 a. Chin Sci Bull, 50: 1512–1522

He S P. 2012. Reduction of the East Asian winter monsoon interannual variability after the mid-1980s and possible cause. Chin Sci Bull, 58: 1331–1338

Jiang Z N, Mu M, Wang D H. 2009. Ensemble prediction experiments using conditional nonlinear optimal perturbation. Sci China Ser D-Earth Sci, 52: 511–518

Li C Y, Li G L. 1999. Variation of the NAO and NPO associated with climate jump in the 1960s. Chin Sci Bull, 44: 1765–1769

Li L, Li C Y, Song J. 2012. Arctic Oscillation anomaly in winter 2009/2010 and its impacts on weather and climate. Sci China Earth Sci, 55: 567–579

Li S L, Wang Y M, Gao Y Q. 2009. A review of the Atlantic Multi-decadal Oscillation (AMO) and its climate influence (in Chinese). Trans Atmos Sci, 32: 458–465

Ma Z G, Fu C B. 2007. Global aridification in the second half of the 20th century and its relationship to large-scale climate background. Sci China Ser D-Earth Sci, 50: 776–788

Mu M, Jiang Z N. 2008. A new approach to the generation of initial perturbations for ensemble prediction: Conditional nonlinear optimal perturbation. Chin Sci Bull, 53: 2062–2068

Sun J Q, Yuan W, Gao Y Z. 2008. Arabian Peninsula-North Pacific Oscillation and its association with the Asian summer monsoon. Sci China Ser D-Earth Sci, 51: 1001–1012

Wang H J, Sun J Q, Fan K. 2007. Relationships between the North Pacific

Oscillation and the typhoon/hurricane frequencies. Sci China Ser D-Earth Sci, 50: 1409–1416
Wei F Y, Zhang T. 2009. Oscillation characteristics of summer precipitation in the Huaihe River valley and relevant climate background. Sci China Ser D-Earth Sci, 53: 301–316
Wu B Y, Huang R H. 1999. Effects of the extremes in the North Atlantic Oscillation on East Asia winter monsoon (in Chinese). Chin J Atmos Sci, 23: 641–650
Wu B Y, Zhang R H, Wang J. 2005. Abnormity of the Arctic Atmosphere dipole mode and the Arctic Sea ice motion in winter (in Chinese). Sci China Ser D-Earth Sci, 35: 184–191
Xu H L, Li J P, Feng Juan, et al 2012. The asymmetric relationship between the winter NAO and the precipitation in Southwest China (in Chinese). Acta Meteorol Sin, 70: 1276–1291
Zhang X J, Jin L Y, Chen C Z, et al. 2011. Interannual and interdecadal variations in the North Atlantic Oscillation spatial shift. Chin Sci Bull, 56: 2621–2627
Zhou B T, Cui X, Zhao P. 2008. Relationship between the Asian-Pacific oscillation and the tropical cyclone frequency in the western North Pacific. Sci China Ser D-Earth Sci, 51: 380–385
Zhou B T, Xia D D. 2012. Interdecadal change of the connection between winter North Pacific Oscillation and summer precipitation in the Huaihe River valley. Sci China Earth Sci, 55: 2049–2057
Croci-Maspoli M, Schwierz C. 2007. Atmospheric blocking: Space-time links to the NAO and PNA. Clim Dyn, 29: 713–725
Davini P, Cagnazzo C, Gualdi S, et al. 2012. Bidimensional diagnostics, variability and trends of Northern Hemisphere blocking. J Clim, 25: 6496–6509
Davini P, Cagnazzo C, Neale R, et al. 2012. Coupling between Greenland blocking and the North Atlantic Oscillation pattern. Geophys Res Lett, 39: L14701
Dong B W, Sutton R T, Woollings T. 2010. Changes of interannual NAO variability in response to greenhouse gases forcing. Clim Dyn, 37: 1621–1641
Hilmer M, Jung T. 2000. Evidence for a recent change in the link between the North Atlantic Oscillation and Arctic sea ice export. Geophys Res Lett, 27: 989–992
Hurrell J W. 1995. Decadal trends in the North Atlantic Oscillation: Regional temperatures and precipitation. Science, 269: 676–679
Hurrell J W. 1996. Influence of variations in extratropical wintertime teleconnections on northern hemisphere temperature. Geophys Res Lett, 23: 665–668
Hurrell J W, Kushnir Y, Ottersen G, et al. 2003. The North Atlantic Oscillation: Climatic significance and environmental impact. Geophys Monogr, 134: 279
Jung T, Hilmer M, Ruprecht E, et al. 2003. Characteristics of the recent eastward shift of interannual NAO variability. Notes Correspond, 16: 3371–3381
Jiang Z N, Mu M, Luo D H. 2013. A study of North Atlantic Oscillation using conditional nonlinear optimal perturbations. J Atmos Sci, 70: 855–875
Kenyon J, Hegerl G C. 2008. Influence of modes of climate variability on global temperature extremes. J Clim, 21: 3872–3889
Kenyon J, Hegerl G C. 2010. Influence of modes of climate variability on global precipitation extremes. J Clim, 23: 6248–6262
Li S L, Bates G. 2007. Influence of the Atlantic Multidecadal Oscillation (AMO) on the winter climate of East China. Adv Atmos Sci, 24: 126–135
Luo D H, Gong T T. 2006. A possible mechanism for the eastward shift of interannual NAO action centers in last three decades. Geophys Res Lett, 33: L24815
Luo D H, Lupo A, Wan H. 2007. Dynamics of eddy-driven low-frequency dipole modes. Part I: A simple model of North Atlantic Oscillations. J Atmos Sci, 64: 3–28
Luo D H, Gong T T, Lupo A. 2007. Dynamics of eddy-driven low-frequency dipole modes. Part II: Free mode characteristics of NAO and diagnostic study. J Atmos Sci, 64: 29–51
Luo D H, Gong T T, Diao Y N. 2007. Dynamics of eddy-driven low frequency dipole modes. Part III: Meridional displacement of westerly jet anomalies during two phases of NAO. J Atmos Sci, 64: 3232–3248
Luo D H, Cha J, Feldstein S B. 2012. Weather regime transitions and the interannual variability of the North Atlantic Oscillation. Part I: A likely connection. J Atmos Sci, 69: 2329–2346
Luo D H, Cha J, Feldstein S B. 2012. Weather regime transitions and the interannual variability of the North Atlantic Oscillation. Part II: Dynamical processes. J Atmos Sci, 69: 2347–2363
Luo D H, Cha J. 2012. The North Atlantic Oscillation and North Atlantic jet variability: Precursors to NAO regimes and transitions. J Atmos Sci, 69: 3764–3787
Mu M, Zhang Z Y. 2006. Conditional nonlinear optimal perturbations of a two-dimensional quasigeostrophic model. J Atmos Sci, 63: 1587–1604
Scherrer S C, Croci-Maspoli M, Schwierz C, et al. 2006. Two-dimensional indices of atmospheric blocking and their statistical relationship with winter climate patterns in the Euro-Atlantic region. Int J Climatol, 26: 233–249
Shabbar A, Huang J P, Higuchi K. 2001. The relationship between the wintertime North Atlantic Oscillation and blocking episodes in the North Atlantic. Int J Climatol, 21:355–369
Sillmann J, Croci-Maspoli M. 2009. Present and future atmospheric blocking and its impact on European mean and extreme climate. Geophys Res Lett, 36: L10702
Tibaldi S, Molteni F. 1990. On the operational predictability of blocking. Tellus, 42: 343–365
Walker G T. 1924. Correlations in seasonal variations of weather IX. Mem Ind Meteor Dept, 24: 275–332
Walker G T, Bliss E W. 1932. World weather V. Mem Roy Meteor Soc, 4: 53–84
Wang C Z, Liu H L, Lee S K. 2010. The record-breaking cold temperatures during the winter of 2009/2010 in the Northern Hemisphere. Atmos Sci Lett, 11: 161–168
Woollings T J, Hoskins B J, Blackburn M, et al. 2008. A new Rossby wave-breaking interpretation of the North Atlantic Oscillation. J Atmos Sci, 65: 609–626
Wu Z W, Li J P, Wang B, et al. 2009. Can the Southern Hemisphere annular mode affect China winter monsoon? J Geophys Res, 114: D11107